

Effect of Temperature on the Interaction between the Nonionic Surfactant C₁₂E₅ and Poly(ethylene oxide) Investigated by Dynamic Light Scattering and Fluorescence Methods

Eloi Feitosa,[†] Wyn Brown,* Marilena Vasilescu,[‡] and Martin Swanson-Vethamuthu

Department of Physical Chemistry, University of Uppsala, Box 532, 751 21 Uppsala, Sweden

Received January 19, 1996; Revised Manuscript Received July 1, 1996[®]

ABSTRACT: The interaction between the nonionic surfactant C₁₂E₅ and a high molar mass ($M = 5.94 \times 10^5$) poly(ethylene oxide) (PEO) in aqueous solution has been examined as a function of temperature by dynamic light scattering and fluorescence methods over a broad concentration range. Clusters of small surfactant micelles form within the PEO coil, leading to its extension. The hydrodynamic radius of the complex increases strongly with temperature as well as with the concentrations of surfactant and polymer. At high concentrations of the surfactant, the coil/micellar cluster complex coexists with free C₁₂E₅ micelles in the solution. Fluorescence quenching measurements show a moderate micellar growth from 155 to 203 monomers in PEO-free solutions of C₁₂E₅ over a wide concentration range (0.02–2.5%) at 8 °C. Below 0.25% C₁₂E₅, the average aggregation number (N) of the micelles is smaller in the presence of PEO than in its absence. However, N increases with increasing surfactant concentration up to a plateau value of about 270 at about 1.2% (ca. 30 mM) C₁₂E₅. At high surfactant concentrations, N is larger in the presence of polymer than in its absence, a finding which is connected to a significant lowering of the clouding temperature due to the PEO at these compositions. Similar results of increasing aggregation number followed by a plateau were also found at a fixed concentration of surfactant (2.5%) and varied PEO.

Introduction

There is increasing interest in ternary surfactant/polymer systems from both theoretical¹ and experimental² points of view. PEO is a favored polymer for such studies due to its unusual solubility properties, but the extension of the knowledge gained to other surfactant/polymer systems is not straightforward. Thus, although the general features of the interactions in various such systems have been extensively examined, it is difficult to delineate general rules since the interactions are strongly system dependent, depending on the hydrophobic/hydrophilic and/or structural and charge characteristics of the components.³ While neutral polymers such as PEO are known to interact comparatively strongly with anionic surfactants, such as sodium dodecyl sulfate (SDS),² they interact only weakly with cationic surfactants such as the alkyltrimethylammonium bromides.^{7–9} However, cationic surfactants form complexes with polymeric acids which are weakly ionized, such as poly(acrylic acid) at low pH.¹⁰ The relative surfactant/polymer composition, and the temperature influence the interaction between surfactant and polymer. The physical properties of the micellar aggregates, such as the cloud point, critical micelle concentration (cmc), and the micellar size (aggregation number),^{4–6} are highly dependent on the relative lengths of the polar and apolar portions of the surfactant, which also determine the strength of interaction with polymers.

The nature and extent of the interactions between neutral polymers and nonionic surfactants have also been controversial and in some aspects are still ambiguous. In an initial approach to this problem, the earlier paper¹¹ dealt with the ternary system containing the

nonionic surfactant C₁₂E₅ and a PEO fraction of high molar mass ($M = 5.94 \times 10^5$). There it was established that, in contrast to the interactions of this polymer with SDS, where a complex is formed in which small micelles are strung along the chain, clusters of small surfactant micelles form within the PEO coil, leading to its extension for steric reasons. Thus, the excluded volume effect resulting on addition of high molar mass polymer to the system drives formation of nonionic surfactant micellar clusters.

The role of the system composition was examined¹¹ and it was found, for example, that on addition of the high molar mass PEO fraction there is a pronounced decrease in the cloud point in comparison with the binary C₁₂E₅–water system. The relatively low clouding temperature of C₁₂E₅ in water (≈ 32 °C), combined with the decreasing polarity of PEO with increasing temperature, makes this system an interesting one for investigating the influence of temperature on the polymer–surfactant interactions.

The present work thus extends the measurements described in the previous paper¹¹ to wider ranges of concentration and in particular focuses on the role of temperature change. Dynamic light scattering (DLS) measurements have been made on the ternary C₁₂E₅–PEO–water system at temperatures varying from 4 °C up to the cloud point (T_c) of the system in two different ways: (1) maintaining consecutively constant each of the solution components and varying the other; and (2) varying the concentration of both the solution components but keeping the ratio (R) between them constant.

Fluorescence probing methods have also been used to obtain additional information regarding the polymer–surfactant interaction, especially on the cmc (or cac) and the micellar aggregation number to examine the variation of the micellar size on addition of polymer to the system. At low concentrations of surfactant, the average aggregation number of the C₁₂E₅ micelles is found to decrease on adding PEO, as already described.¹¹

[†] Permanent address: Departamento de Física, IBILCE/UNESP, São José do Rio Preto, SP, Brazil.

[‡] Permanent address: Institute of Physical Chemistry, Romanian Academy, Spl. Independentei Nr. 202, Bucharest, Romania.

[®] Abstract published in *Advance ACS Abstracts*, September 15, 1996.

Materials and Methods

C₁₂E₅ (pentaethylene glycol mono-*n*-dodecyl ether) was purchased from Nikko Chemicals, Japan, and PEO ($M_w = 5.94 \times 10^5$ g/mol; $M_w/M_n = 1.03$) was from Toyo Soda, Ltd., Japan, and used without purification. The cmc of C₁₂E₅ is $2.64 \times 10^{-3}\%$ (w/w) (65 μ M) at 25 °C.⁴ Concentrations of the surfactant are expressed either in % (w/w) or moles/liter (M) (1% of C₁₂E₅ corresponds to 24.6 mM).

Pyrene and 3,4-dimethylbenzophenone 99% (DMBP), from Aldrich, were recrystallized from ethanol. Probes and quencher were transferred from stock solutions to empty flasks and the solvent evaporated. The surfactant or surfactant-polymer solutions were then added and the mixtures were magnetically stirred. Measurements were performed after 24 h to ensure that equilibrium was attained. The pyrene concentration was kept below 10^{-6} M to avoid excimer formation. The quencher concentration was such that it approximated one DMBP molecule per aggregate and ranged between 10^{-5} and 10^{-4} M.

Dynamic Light Scattering Measurements. DLS measurements were made using the apparatus described briefly in ref 12. An ALV wide-band, multi- τ , digital autocorrelator was used for data collection. The measured intensity autocorrelation function $g_2(t)$ is related to the field correlation function $g_1(t)$ by

$$g_2(t) = B[1 + \beta|g_1(t)|^2]$$

where β is a factor accounting for deviations from ideal correlation and B is a baseline term.

For a continuous distribution of relaxation times, corresponding to an infinite range of particle sizes, the inverse Laplace transform (ILT) may be used:

$$g_1(t) = \int_0^\infty A(\tau)e^{-t/\tau} d\tau$$

ILT analysis was performed using a constrained regularization routine, REPES.¹³ Although similar to CONTIN,¹⁴ the algorithm REPES differs in that it directly minimizes the sum of the squared differences between the experimental and calculated intensity-intensity autocorrelation functions $g_2(t)$ using nonlinear programming and allows the selection of the "smoothing parameter" P (probability to reject).¹⁵ Analysis of data encompassing 288 exponentially spaced grid points and a grid density of 12 per decade can be rapidly performed on an IBM AT desk top computer. Representation of the relaxation time distributions in the form of a $\tau A(\tau)$ versus $\log \tau$ plot, with $\tau A(\tau)$ in arbitrary units, provides an equal-area representation.

Fluorescence Measurements. Time-resolved fluorescence decay data were collected by means of the single-photon-counting technique. Fluorescence excitation was achieved by a Nd-YAG mode-locked laser which pumped a dye laser (DCM as dye and a KDP crystal for frequency doubling). The excitation and emission wavelengths, selected by monochromators, were 320 and 395 nm, respectively. The technique and data analysis are described elsewhere.¹⁶⁻¹⁸ Fluorescence steady-state spectra were recorded on a SPEX Fluorolog 1680 combined with a SPEX Spectroscopy Laboratory Coordinator DM1B. Measurements were carried out at controlled temperatures, in air-equilibrated solutions.

The time-resolved fluorescence quenching method (TRFQ) in microheterogeneous solutions is well described in the literature¹⁹⁻²¹ and is based on the equation²²

$$\ln[F(t)/F(0)] = -A_2 t + A_3[\exp(-A_4 t) - 1] \quad (1)$$

where $A_2 = k_0 + k_q k_- n / (k_q + k_-)$, $A_3 = n k_q^2 / (k_q + k_-)^2$, and $A_4 = k_q + k_-$, k_q standing for the first-order quenching rate constant, k_- for the exit rate constant of a quencher leaving the micelle, and n for the average number of quenchers per micelle.

If k_- is much less than k_q and k_0 , eq 1 becomes

$$\ln[F(t)/F(0)] = -k_q t + n[\exp(-k_q t) - 1] \quad (2)$$

This is the ideal case for determination of the aggregation

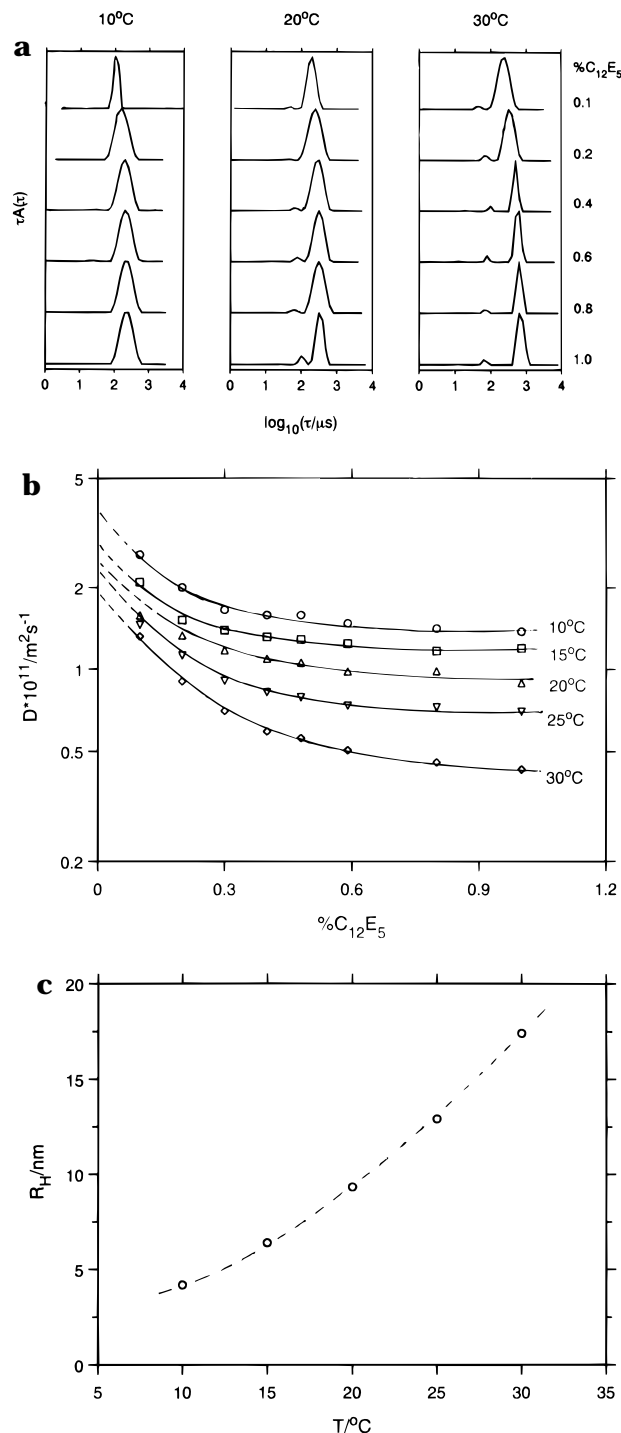


Figure 1. (a) Relaxation time distributions using ILT for binary C₁₂E₅ aqueous solutions at different surfactant concentrations and at three temperatures. Data at angle 90°. (b) Translational diffusion coefficients versus concentration for the binary C₁₂E₅/water system at the temperatures indicated. (c) Hydrodynamic radii for the binary C₁₂E₅ system as a function of temperature.

number. Fitting the experimental data to eq 2 yields the values of n and k_q . The aggregation number (N) is given by

$$N = n[S]_{\text{mic}}/[Q]_{\text{mic}} \quad (3)$$

where $[S]_{\text{mic}}$ and $[Q]_{\text{mic}}$ are the surfactant and quencher concentrations in the micelles, respectively; $[S]_{\text{mic}} = [S]_t - [S]_f$, where $[S]_t$ is the total surfactant concentration. One usually considers $[S]_f = [S]_{\text{cmc}}$. Because DMBP has a low solubility in water, the quencher concentration in the micelles is corrected

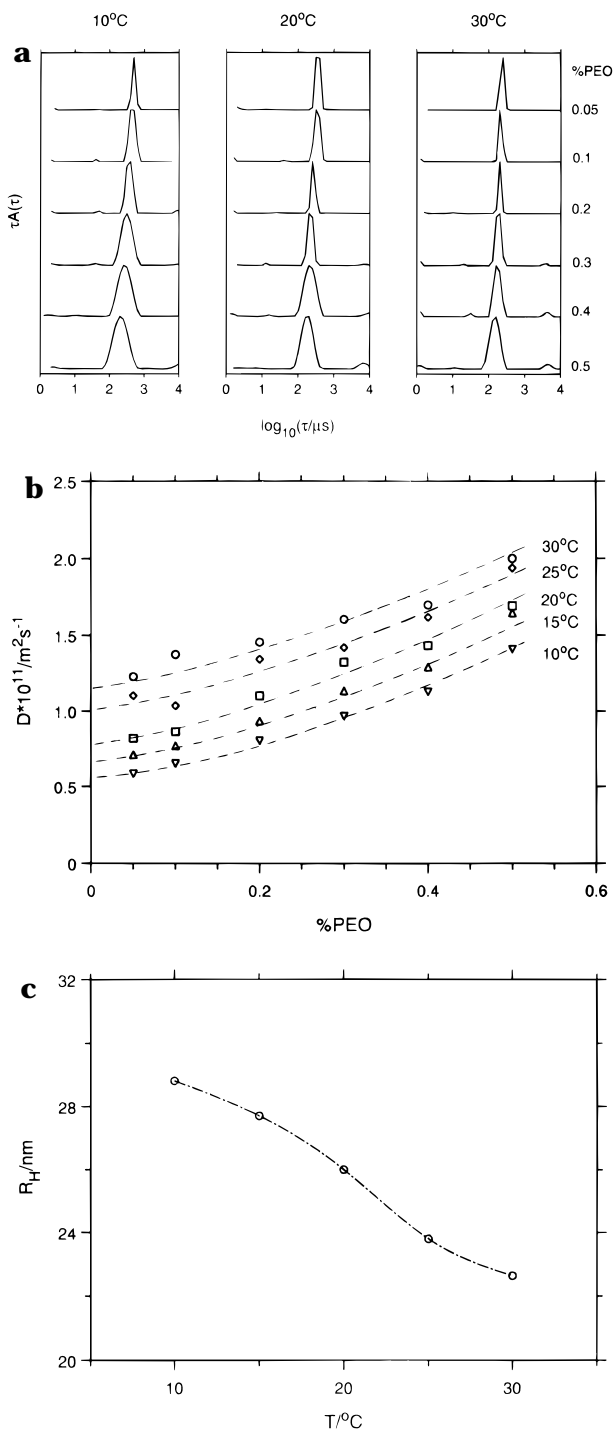


Figure 2. (a) Relaxation time distributions (ILT) for the binary PEO/water system at the different PEO concentrations and temperatures indicated. (b) Diffusion coefficients versus concentration for the binary PEO/water system at the temperatures indicated. (c) Temperature dependence of the hydrodynamic radius for the binary PEO/water system as a function of temperature.

by the equation

$$[Q]_{\text{mic}} = [Q]_{\text{t}} \{k_D[S]_{\text{mic}}\} / \{k_D[S]_{\text{mic}} + 1\} \quad (4)$$

where $[Q]_{\text{t}}$ is the total quencher concentration and k_D the rate constant for DMBP distribution between the micelles and the aqueous phase. The value of k_D for DMBP in 1% C₁₂E₅ was determined as 2525 M^{-1} at 10 °C by the method described in ref 23 and used in the analysis.

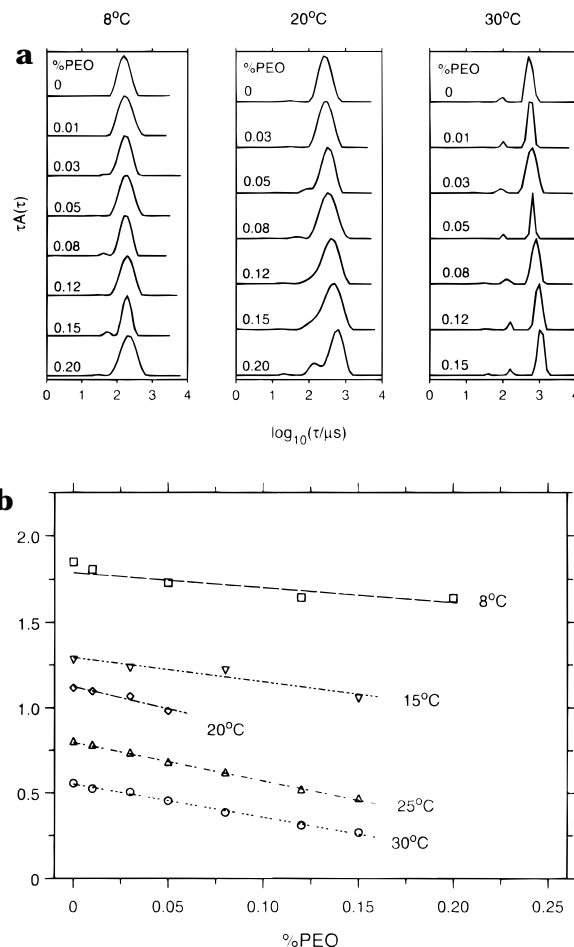


Figure 3. (a) ILT relaxation time distributions for the ternary C₁₂E₅/PEO/water system at a constant surfactant concentration of 0.5%. The data are at the PEO concentrations and temperatures shown. (b) Diffusion coefficients for the ternary system in (a), at the temperatures shown, plotted versus PEO concentration.

Results and Discussion

Binary Systems. Figure 1a shows relaxation time distributions obtained from the autocorrelation functions by ILT using REPES (see Experimental Section) for binary C₁₂E₅ solutions at three temperatures. The distributions are close to single exponential at 10 °C but, as noted previously,¹¹ contain a low-amplitude component with short relaxation time at 20 and 30 °C which is enhanced in intensity at higher surfactant concentration. The strongly decreasing value of the translational diffusion coefficient for the main peak ($D = \Gamma/q^2$ with Γ the relaxation rate $= \tau^{-1}$ and q the scattering vector) is shown as a function of surfactant concentration in the log–lin plot in Figure 1b. The strong curvature in the concentration range below about 0.5% was earlier interpreted^{11,24,25} as deriving from micellar growth/intermicellar interactions. Approximate values of the hydrodynamic radii (R_H) were obtained from the estimated zero-concentration value of D at each temperature using the Stokes–Einstein equation:

$$R_H = kT/6\pi\eta_0 D_0 \quad (5)$$

and this parameter is shown in Figure 1c as a function of temperature. The solvent viscosity at the relevant temperature, η_0 , has been used in eq 5. Kato et al.²⁵ found that the correlation length, similarly estimated but for concentrations above the overlap concentration, also increases with increasing temperature.

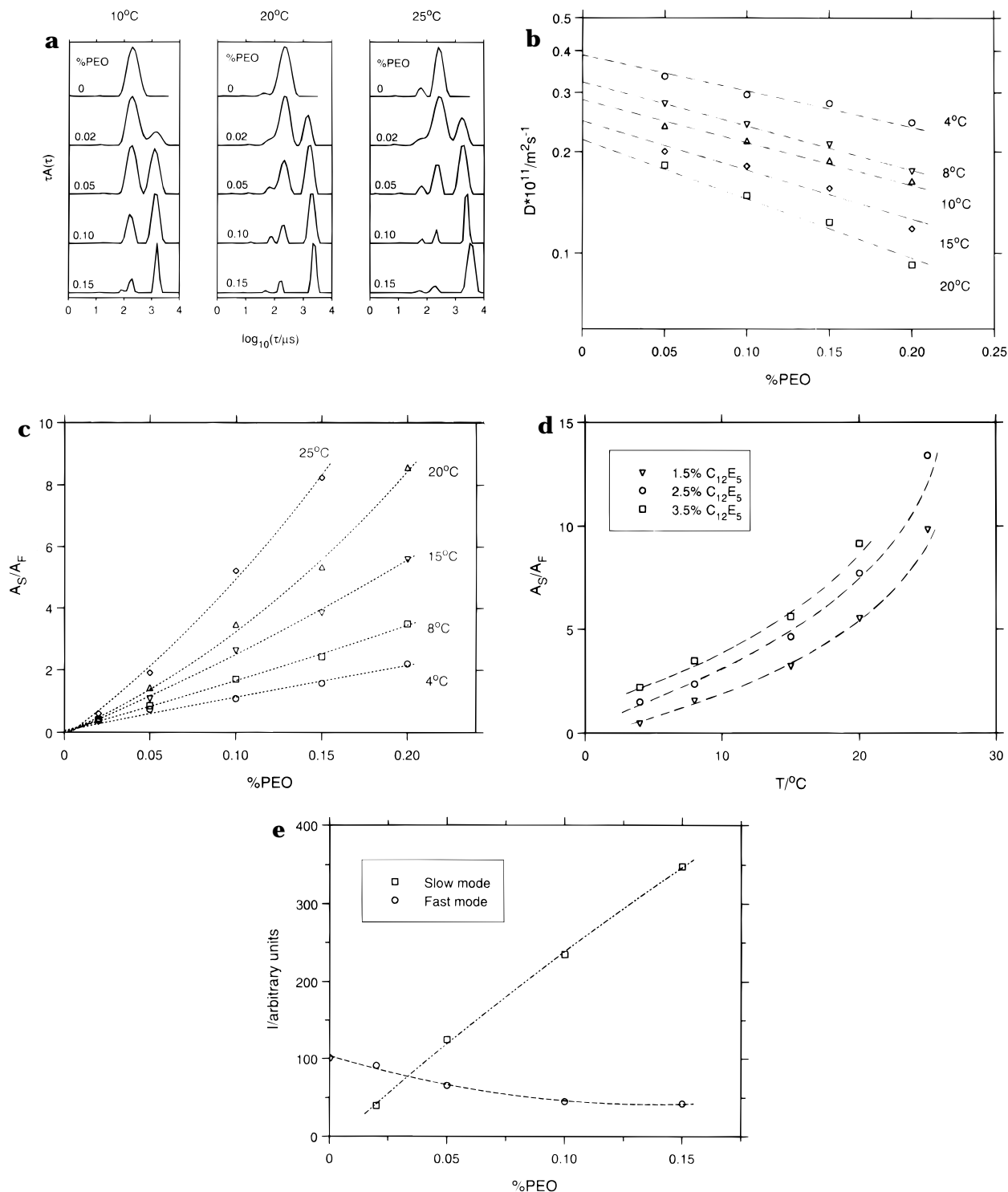


Figure 4. (a) ILT relaxation time distributions similar to those in Figure 3a, but at a constant surfactant concentration of 3.5%. The distributions are shown at different PEO concentrations and temperatures as indicated. (b) Diffusion coefficients plotted versus PEO concentration for a constant surfactant concentration of 3.5% at the temperatures indicated. (c) The intensity of the slow cluster mode and the fast micellar mode as a function of the PEO concentration at C (surfactant) = 3.5% and 25 °C. (d) Variation of the DLS amplitude ratio of slow to fast modes with temperature at the concentrations of surfactant shown in the insert and concentration PEO of 0.1%. (e) DLS measurements: intensities of slow and fast modes as a function of PEO concentration for surfactant concentration 3.5% at 25 °C.

Figure 2a shows examples of ILT relaxation time distributions for the PEO fraction in dilute solution at three temperatures. The single-coil diffusion coefficients derived from the peak moments are shown as a function of concentration in Figure 2b.

Hydrodynamic radii estimated from the intercepts using eq 5 are shown in Figure 2c as a function of temperature. R_H decreases with increasing temperature in the range 8–30 °C. This behavior is well known

for PEO in aqueous solution and is understood to derive from the more compact conformation adopted by the oxyethylene chain at elevated temperature due to a higher population of unfavorable states.²⁶

Ternary Systems. Figure 3a shows ILT results at three temperatures for the ternary PEO– $C_{12}E_5$ –water solutions at a constant $C_{12}E_5$ concentration of 0.5% and with increasing PEO concentration. The distributions are essentially single modal at 8 and 20 °C and then

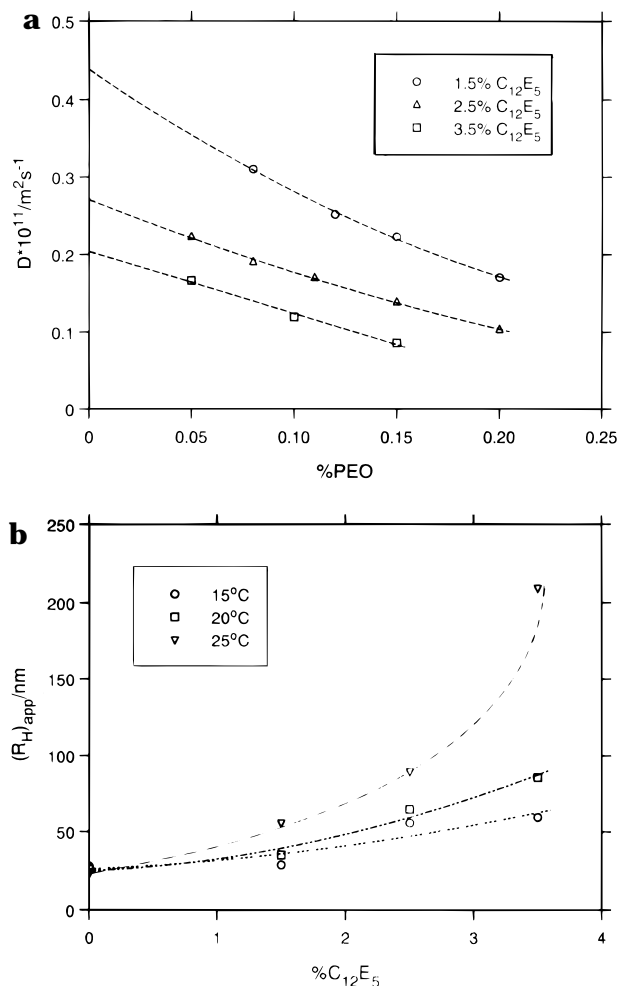


Figure 5. (a) Diffusion coefficients for the coil/cluster complex in the ternary system as a function of the PEO concentration, maintaining the surfactant concentration at fixed levels as indicated. Data are at 25 °C. (b) Apparent hydrodynamic radii estimated from the intercepts in (a) showing the dependence on surfactant concentration at the temperatures shown.

shift progressively to a longer relaxation time with increasing PEO concentration at 30 °C. At the higher PEO concentrations and 20° the main peak is asymmetric owing to overlap with an emerging faster component. At 30 °C a low intensity fast peak accompanies the main peak. As previously concluded,¹¹ the main peak most likely derives from clusters of micelles formed due to the excluded volume effect of the high molar mass PEO component present in the solution. These micellar clusters are stabilized within the PEO coil and lead to its swelling. The fast mode which is seen most clearly at 30 °C, corresponds to free surfactant micelles, as deduced from the hydrodynamic radius.

Figure 3b depicts the diffusion coefficients corresponding to the main peak in Figure 3a as a function of PEO concentration at different temperatures. The points included for zero PEO concentration are data interpolated at the surfactant concentration of 0.5% in Figure 1b for the binary surfactant system. It is noted that temperature strongly influences the D -value, while the approximately constant negative slope suggests a weak attractive interaction between the complex particles which is of similar magnitude over the temperature interval examined.

Figure 4a shows analogous ILT results to those in Figure 3a but here they refer to a fixed surfactant concentration of 3.5%. A similar overall pattern is

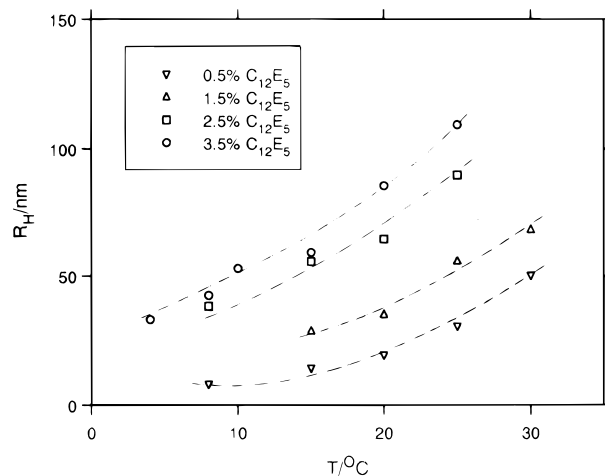


Figure 6. Hydrodynamic radius of the coil/cluster complex as a function of temperature at the surfactant concentrations (bottom to top) 0.5, 1.5, 2.5, and 3.5%.

discernible but the development of the free micellar mode amplitude with increasing PEO concentration is more pronounced. Linear relationships (not shown) between the peak relaxation rate Γ and q^2 were obtained for the two main modes demonstrating diffusive processes. The C₁₂E₅ free micellar peak has an essentially unchanged relaxation time with increasing PEO concentration, whereas the slow "micellar cluster" peak increases in relaxation time with increasing PEO concentration at each temperature. The fast satellite peak of low amplitude becomes increasingly important with increasing temperature both for the pure surfactant and in the ternary solutions and also has an unchanged relaxation time with change in PEO concentration.

Diffusion coefficients for the slowest mode in Figure 4a are shown as log–lin plots in Figure 4b as a function of PEO concentration at different temperatures. Figures 4c,d show how the slow cluster mode becomes increasingly dominant with change in PEO concentration and temperature.

The interpretation placed on the above results follows that advanced in the prior publication.¹¹ There it was concluded that clusters of surfactant micelles form within the PEO coil and thereby lead to its expansion: when the surfactant concentration is reduced, the coil radius progressively decreases and finally attains the value found in the absence of surfactant, i.e. that found in the binary PEO/water system. It is important to note that, while the C₁₂E₅ micelles are observed to grow strongly forming asymmetric structures with increasing concentration and temperature in their binary solutions as is shown in Figure 1b,c, micellar clusters are not observed in the binary solutions: this is true at all temperatures up to the cloud point at about 32 °C. Cluster formation is a phenomenon only found in the ternary system in the presence of the large PEO coils which, through the excluded volume effect, drive cluster formation in the surfactant system. Figure 4e shows the enhancement of the absolute intensity of the cluster mode at different PEO concentrations at a constant concentration of C₁₂E₅ = 3.5%, and this contrasts with the approximately constant intensity of the free micellar peak.

Diffusion coefficients at three constant C₁₂E₅ concentrations are extrapolated to infinite dilution PEO in Figure 5a. From the intercepts, the apparent coil dimension (R_H) at finite C₁₂E₅ concentrations has been estimated using eq 5. These radii are summarized in

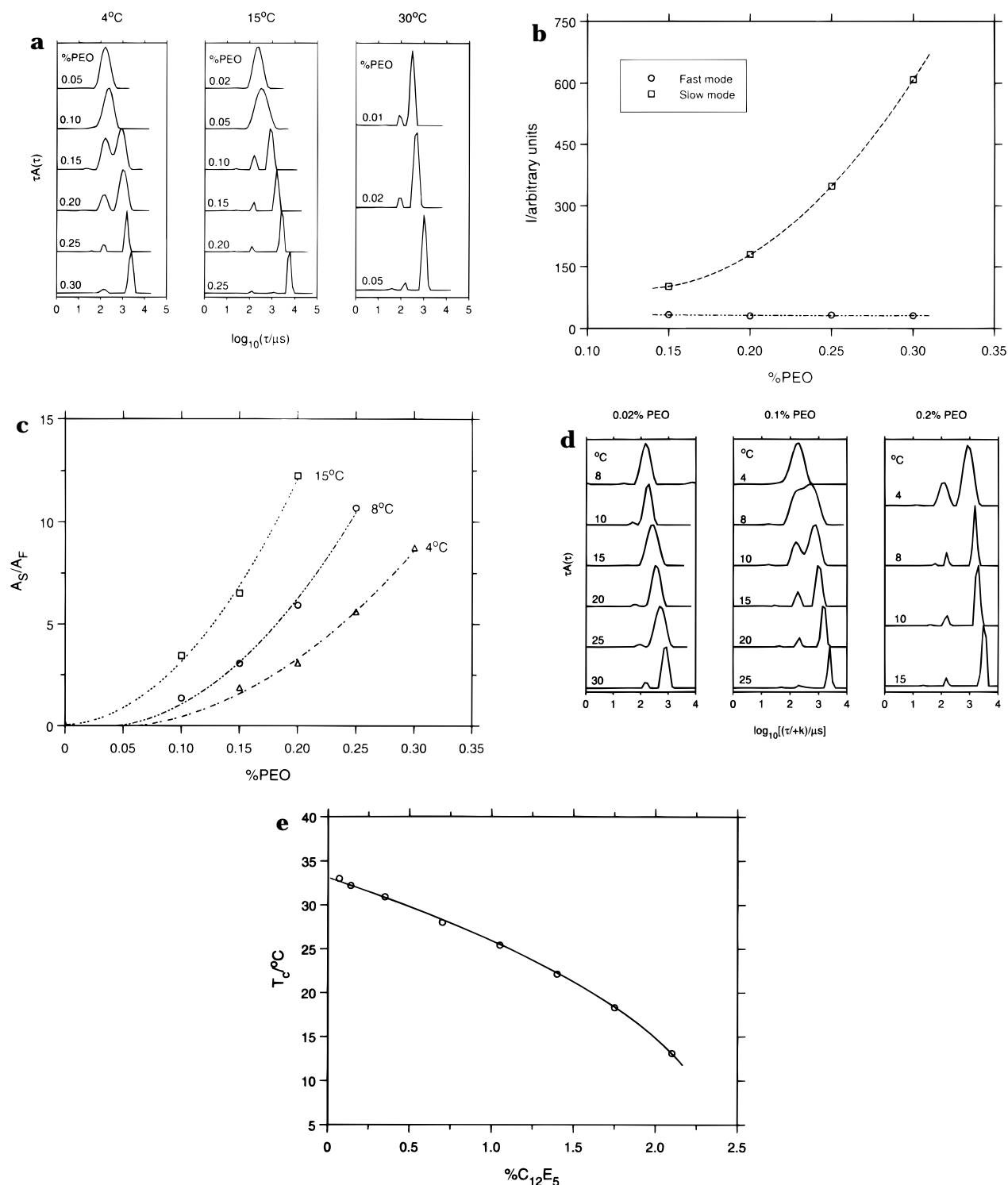


Figure 7. (a) ILT relaxation time distributions for data obtained at a constant surfactant/polymer ratio $R = 7$. The polymer concentration is indicated. (b) Intensity of fast and slow modes in (a) as a function of PEO concentration for constant surfactant/PEO ratio $R = 7$ at 8°C. (c) Effect of PEO concentration on the ratio between the slow and fast mode amplitudes at constant surfactant/polymer ratio $R = 7$ and the temperatures shown. (d) Relaxation time distributions (ILT) at different temperatures and concentrations of PEO for $R = 7$. The log(time) axis has been shifted by the factor (T/η) to facilitate comparison. (e) The variation in the clouding temperature (T_c) with surfactant concentration at surfactant/PEO ratio $R = 7$.

Figure 5b as a function of surfactant concentration at 8, 25, and 30°C. These data would indicate that (a) the coil expands as the surfactant concentration increases and also that (b) the coil expansion is greater the higher the temperature. Data points at zero surfactant concentration are taken from Figure 2c for the binary PEO system.

Figure 6 shows the corresponding trends in the apparent R_H for the PEO/micellar cluster complex with

change in temperature for selected concentrations of C₁₂E₅. These data demonstrating coil expansion, taken together, substantiate the earlier interpretation¹¹ of micellar clustering within the polymer coil.

Constant Surfactant/Polymer Ratio. Complementary measurements were also made on the ternary system at a constant ratio $R = \text{C}_{12}\text{E}_5/\text{PEO} = 7$ as a function of temperature. Figure 7a shows ILT results for various PEO concentrations at three temperatures.

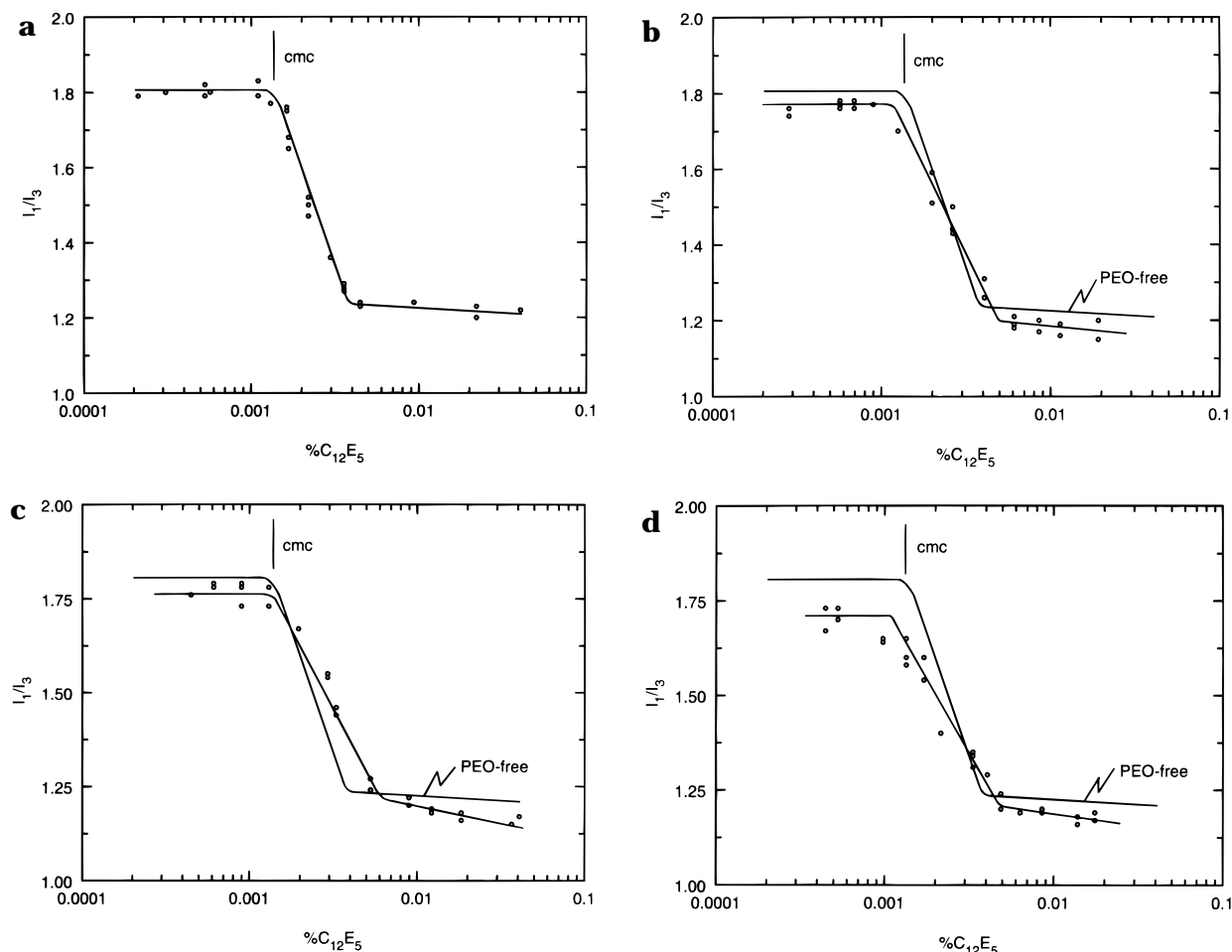


Figure 8. Fluorescence intensity ratio between the first and third vibronic peaks (I_1/I_3) as a function of surfactant concentration at 22 °C: (a) in the absence of polymer and in the presence of (b) 0.05%, (c) 0.1%, and (d) 0.2% PEO. The curve in (a) (without the points) is superimposed for comparison purposes in (b), (c), and (d).

The peak corresponding to free micelles has an approximately constant relaxation time when the PEO concentration is increased at each temperature, and the intensity of this component is independent of the PEO concentration (Figure 7b). Figure 7c depicts the effect of temperature on the A_S/A_F ratio: the higher the temperature, the more dominant is the complex (slow) mode.

Figure 7d shows how the relaxation time distributions change with temperature at three constant PEO concentrations at $R = 7$. The $\log(\text{time})$ axis has been shifted by the factor $k = (T/\eta)$ to facilitate comparison. Temperature change affects the relaxation time of the slow mode more than the fast mode: the relative amplitude of the fast mode decreases with increasing temperature. There is a stronger temperature effect than observed at a C₁₂E₅ concentration of 3.5% shown in Figure 4e.

Measurements of the clouding temperature were made at constant ratio surfactant/polymer = 7 as a function of the surfactant concentration. These data are summarized in Figure 7e. T_c decreases strongly with increasing C₁₂E₅ concentration.

Steady-State Fluorescence Measurements. The fluorescence intensity ratio between the first and third vibronic peaks (I_1/I_3) of excited state monomeric pyrene emission was determined over a wide range of C₁₂E₅ concentration (0.004–0.04%) both in the absence of PEO (Figure 8a) and in the presence of 0.05% PEO (Figure 8b) at 22 °C. Similar determinations were also made at 0.1% (Figure 8c) and 0.2% PEO (Figure 8d). The

variations in the vibrational fine structure of pyrene monomer emission has been widely used as a spectroscopic tool to study micellar properties.²¹ The change in the characteristic I_1/I_3 ratio (with and without PEO) indicates that the surfactant micelles do not interact directly with the PEO coils. However, the results of the static fluorescence measurements show that the interaction increases with increase in PEO concentration, although the precise nature of the interaction remains unclear.

(a) The value of I_1/I_3 depends on the PEO concentration. At low surfactant concentrations (below the cmc) the ratio is lower for the polymer-containing solutions (lowest for the highest polymer content) than for the polymer-free samples, suggesting that pyrene "senses" a less polar medium in the presence of PEO.

(b) After micellization begins, pyrene is increasingly partitioned into the hydrophobic domains leading to a sharper decrease in the I_1/I_3 ratio for the polymer-free case. For polymer-containing solutions, the decrease is less steep and is dependent on the PEO concentration (i.e. the concentration interval of the slope increases with increase in PEO). This behavior reveals the existence of interactions between PEO and C₁₂E₅. Similar results have been observed for interactions with PEO and cationic surfactant.⁸ Taking the cmc or cac as the concentration at which the ratio starts to decrease (as is usual for nonionic surfactants), no significant dependence of the cac on adding PEO was noted. However, changes in the slope of the curve above the cmc or cac probably reflect the extent of interaction felt

by the probe (i.e. progressive changes are slower and are shifted to higher surfactant concentrations in solutions with PEO).

(c) At higher surfactant concentrations, i.e. above about 0.004%, the ratio I_1/I_3 is only marginally lower for the polymer-free solution, showing that the probe senses an approximately constant hydrophobicity in the micelles. The decrease in I_1/I_3 with increasing surfactant concentration, on the other hand, is stronger for the higher PEO-containing solutions; i.e. the polymer increases the hydrophobicity of the pyrene microenvironment somewhat. One could speculate from these and the earlier DLS results that the micelles associated with the coils are probably more compact (compressed) and have a slightly decreased water content in the micellar core compared to the micelles in solutions without polymer. The I_1/I_3 ratio is found to remain constant when the surfactant concentration is fixed at 2.5% (w/w) and the polymer concentration varied within the range 0.01–0.15% (w/w).

Time-Resolved Fluorescence Quenching Measurements. The fluorescence quenching studies were performed with solutions containing a constant concentration of surfactant ($C_{12}E_5$; 2.5%) with varied PEO (0.01–0.15%) and constant PEO (0.1%) and varied $C_{12}E_5$ (0.027–2.5%) mainly at 8 °C and in some cases at 15 °C. Complementary DLS measurements were also performed at 8 °C on the series of compositions used for fluorescence studies and the results are shown in panels A and B of Figure 9a as relaxation time distributions for comparison.

The fluorescence lifetime of pyrene (τ_0) in micellar solutions estimated from the unquenched decay curves is shown as a function of increasing surfactant concentration both with and without 0.1% PEO at 8 °C in Figure 9b. Although the data points scatter somewhat, the results indicate that τ_0 does not change significantly on addition of PEO but is only marginally higher for solutions with PEO (224–230 ns) as opposed to 220–230 ns for PEO-free samples in line with the slight decrease in the I_1/I_3 ratio found in polymer-containing solutions above the cmc (Figures 8b–d). The small increase in lifetime suggests a slightly better shielding of micelle-solubilized pyrene associated with the PEO chains. At higher surfactant concentrations ($\geq 1.5\%$), τ_0 remains nearly constant (228 ± 3 ns) in the polymer and polymer-free solutions showing no particular shielding effects. Increasing the temperature to 15 °C did not show significant differences in pyrene lifetime for the above two cases but instead gave a nearly constant lifetime of 200 ± 3 ns (figure not shown). The corresponding τ_0 for solutions with fixed $C_{12}E_5$ (2.5%) and varied PEO was found to lie between 230–236 ns at 8 °C. The lack of sharp variations in the lifetime data suggests that pyrene senses a similar micellar microstructure and packing within the composition ranges studied. Typical TRFQ decay curves from micelles with probes and with different quencher concentrations are shown in Figure 10a (upper panel, without PEO; right panel, with PEO). Curve 1 is for micelles with only probe molecules while in curves 2 and 3, the initial rapid quenching is from micelles with both probe and quencher followed by a linear exponential tail at long times for micelles with only pyrene present. The decays were also recorded using a longer time window of 2 μ s to check for quenching of excited-state pyrene in quencher-free micelles by quencher molecules migrating from neighboring micelles or the bulk phase, but no signifi-

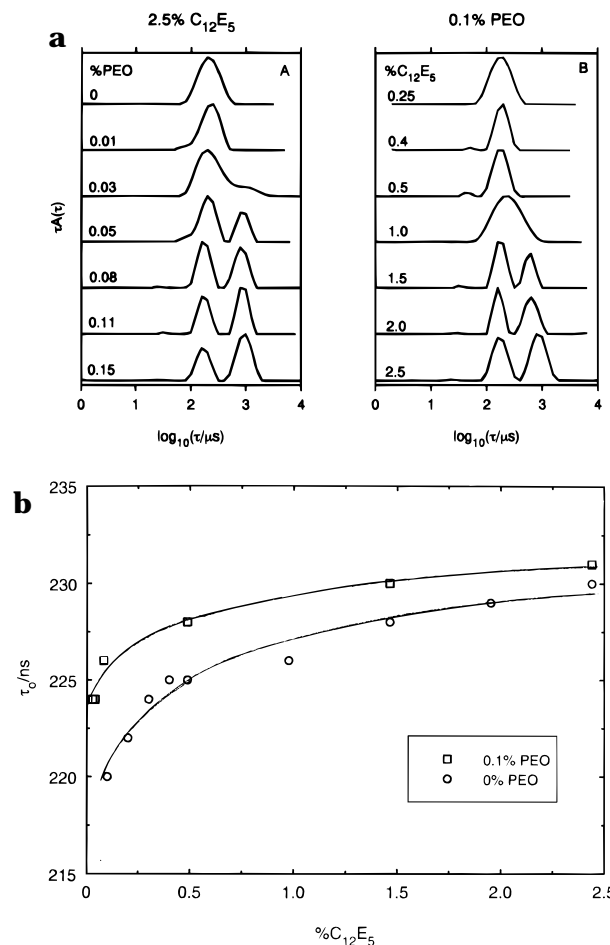


Figure 9. (a) ILT relaxation time distributions from DLS at 8 °C, showing the free micellar component and the coil/cluster complex development with PEO (panel A) and $C_{12}E_5$ concentration (panel B), keeping one of the respective components fixed. (b) Fluorescence lifetime (τ_0) spanning over a wide range of surfactant concentration in the absence and presence of 0.1% PEO at 8 °C.

cant migration effects were detected.

The decay curves were fitted to the model of eqs 1 and 2. The results are shown in Figures 10b and 10c as average aggregation number (N) versus the surfactant concentration with and without 0.1% PEO and similarly in Figure 10d for samples with constant $C_{12}E_5$ but varied PEO concentration at $T = 8$ °C. The results presented in Figures 10b and 10c can be divided into two concentration zones for clarity: At low $C_{12}E_5$ concentrations (i.e. between 0.02 and 0.25%), the N of polymer-associated micelles is smaller than or equal to those in the corresponding PEO-free samples (i.e. within the micellar clusters inside or at the interface of the PEO coils). Similar results were also obtained at 15 °C (not shown) and 20 °C¹¹. The smaller size of the micelles is due to the relatively stronger polymer–surfactant interaction at low concentrations arising mainly from steric effects and restrictions imposed by the PEO chain configuration in water. The DLS results shown in Figure 9a show that these samples are from a region characterized by a unimodal relaxation time distribution where the slightly more hydrophobic environment provided by the PEO coils compared to water favors association of $C_{12}E_5$ micelles mainly due to the excluded volume effect. Initially, the micelles are smaller in size compared to free micelles but grow with increasing surfactant to a similar size at 0.25% $C_{12}E_5$. We note that in a parallel study of the ternary system

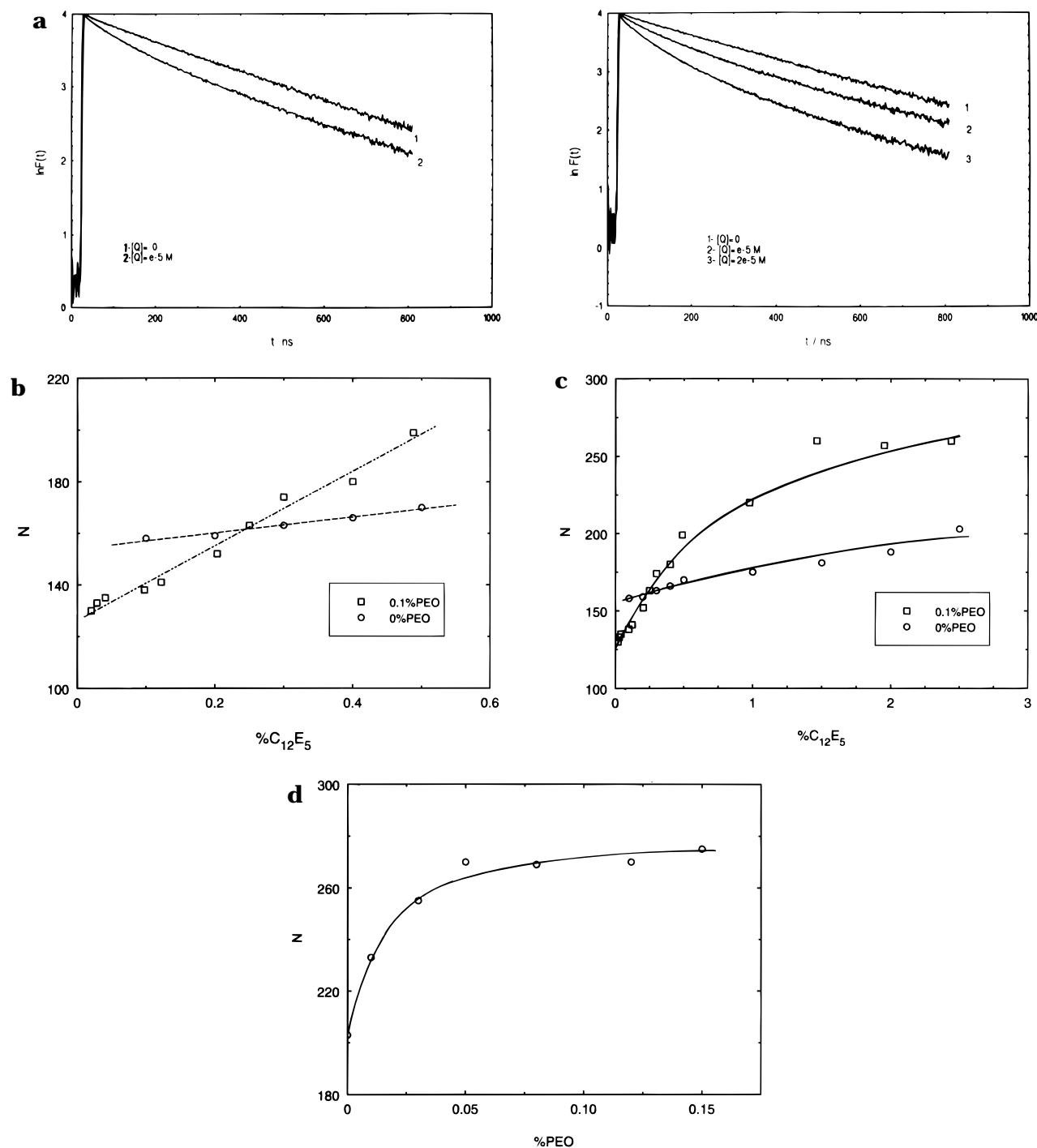


Figure 10. (a) Typical fluorescence decay curves for the $C_{12}E_5$ /PEO system at 8 °C: (left) in the absence of PEO; (right) in the presence of PEO. (b) Dynamic fluorescence data. Average aggregation number (N) as a function of surfactant concentration, with and without polymer (0.1% PEO), at 8 °C. (c) Variation of the average aggregation number with surfactant concentration over an extended range of $C_{12}E_5$ concentration; PEO concentration = 0.1%, 8 °C. (d) Variation of the average aggregation number as a function of increasing PEO concentration at a fixed surfactant concentration of 2.5%; data at 8 °C.

of the cationic surfactant CTAB and essentially neutral poly(acrylic acid) at low pH,³¹ a lower N was found in the presence of the polymer. Figure 10c includes the variation of N for higher concentrations of $C_{12}E_5$ (0.3 to 2.5%) where the average N increases rapidly up to a plateau value of 270 monomers at 1.5% surfactant for the compositions containing 0.1% PEO at 8 °C. This large growth in the PEO-associated micelles (170–270) as opposed to the moderate growth found in polymer-free samples (155–203) can be connected to a significant lowering of the clouding temperature (about 3–4 °C) due to the presence of 0.1% PEO at surfactant concentrations above 0.25%.¹¹ Furthermore, the DLS results

show that at concentrations above 1% $C_{12}E_5$ the broad relaxation time distribution becomes bimodal; this is attributed to a distribution of free $C_{12}E_5$ micelles (the faster mode) and a complex (PEO coils saturated with $C_{12}E_5$ micelles, slower mode). The micelles grow dramatically up to 1.5% $C_{12}E_5$, above which the onset of complex formation and the appearance of the free micellar peak in DLS (Figure 9a(B)) corresponds to a plateau value of N , i.e. 270 monomers (Figure 10c). The increase in aggregation number up to a plateau value is also due to the tendency for new surfactant molecules to prefer to pack in the environment of near-saturated PEO chains (both PEO and $C_{12}E_5$ become more hydro-

phobic as temperature increases; the saturation $C_{12}E_5$ concentration lies between 1.0 and 1.5%). A combination of the above two effects is probably responsible for the dramatic increase and leveling off of the aggregation number above 0.3%. Fluorescence studies do not show two different pyrene lifetimes arising from probe molecules in different microenvironments (free and polymer-associated micelles) but instead give a single pyrene lifetime and an average aggregation number. The result implies that a similar environment with respect to packing and microstructure is felt by the solubilized pyrene molecules at all compositions under study (both bimodal and unimodal distributions).

Figure 10d gives N for solutions with constant $C_{12}E_5$ concentration of 2.5% (60 mM). Again N initially increases on addition of PEO and finally attains a plateau value of about $N \approx 270$. Thus the interaction between PEO and $C_{12}E_5$ is strongly dependent on the concentration of both components as observed previously.¹¹ With 2.5% $C_{12}E_5$ and different PEO concentrations, the micelles are more polydisperse and N depends on the quencher concentration used. For this particular result, N varies with an uncertainty range of 10–15%. The variation in N has been considered at a constant surfactant/quencher concentration ratio throughout. From DLS (Figure 9a, panel A) for the samples with fixed 2.5% $C_{12}E_5$, the distribution is unimodal and broad up to 0.01% PEO, above which a second slower mode is observed at 0.03% PEO. At PEO concentrations of 0.05% and above, the distribution is clearly bimodal as it is above 1.5% $C_{12}E_5$ with fixed PEO (panel B).

Concerning the values of the first order quenching rate constant (k_q), it is known²¹ that k_q is inversely proportional to N for spherical micelles. The present experiments show that k_q varies from 7.5×10^6 to 4.0×10^6 s⁻¹ for polymer-free samples as the surfactant concentration increases from 0.1% to 2.5% at 8 °C. However, in the presence of PEO, k_q is practically constant: 8.4×10^6 s⁻¹ to 7.6×10^6 s⁻¹, up to 0.25% $C_{12}E_5$ at the same temperature. Above 0.3% $C_{12}E_5$, the PEO-containing solutions show a small decrease in the k_q value compared to the PEO-free case, in agreement with the increase in N found in this range and with the behavior found for other surfactant–polymer systems.^{27–30}

Conclusions

The present results from DLS and fluorescence measurements at different temperatures and concentrations of the components confirm the model for neutral polymer–surfactant interaction proposed in the previous communication:¹¹ i.e. micellar clusters are formed within the large PEO coils, leading to coil expansion. The overall hydrodynamic size of the coil/micellar cluster complex increases strongly with increasing temperature up to the clouding point and also with increasing concentration of each component. Above the saturation concentration, the complex co-exists with free micelles in solution.

From the fluorescence measurements, we conclude the following: In dilute solution, high molar mass PEO interacts with polar moieties of the surfactant molecule. The cmc or cac of the surfactant remains unchanged with increase in PEO concentration. At low surfactant concentrations, the aggregation number (N) of the $C_{12}E_5$ micelles within the clusters is smaller than in the polymer-free solution in the temperature range from 8 to 15 °C due to steric factors. N increases with increas-

ing surfactant concentration in the presence of constant PEO concentration, to a plateau value of about 270. N also increases in a similar way with PEO concentration at constant surfactant concentration to approximately the same value. N for the micelles forming the clusters may be smaller or larger than that of the polymer-free micelles depending on the T_c of the system.

Acknowledgment. This work has been financially supported by the Swedish Technical Research Council (TFR). E.F. thanks the Conselho Nacional de Desenvolvimento Científico e Tecnológico (CNPq) for a stipend (Grant 201720/93-0). M.V. is grateful to the Swedish Institute for financial support. M.S.V. gratefully acknowledges helpful discussions with Dr. Elouafi Alami.

References and Notes

- (1) Nikas, Y. J.; Blankschtein, D. *Langmuir* **1994**, *10*, 3512.
- (2) Lindman, B.; Thalberg, K. In *Interactions of Surfactants with Polymers and Proteins*; Goddard, E., Ananthapadmanabhan, K. P., Eds.; CRC Press: Boca Raton, FL, 1993; p 203.
- (3) Goddard, E. D. In *Interactions of Surfactants with Polymers and Proteins*; Goddard, E., Ananthapadmanabhan, K. P., Eds.; CRC Press: Boca Raton, FL, 1993; p 219.
- (4) Degiorgio, V. In *Physics of Amphiphiles: Micelles, Vesicles and Microemulsions*; Degiorgio, V., Corti, M., Eds.; North-Holland: Amsterdam, 1985; p 303.
- (5) Brown, W.; Zhou, P.; Rymdén, R. *J. Phys. Chem.* **1988**, *92*, 6086.
- (6) Nilsson, P.-G.; Wennerström, H.; Lindman, B. *J. Phys. Chem.* **1983**, *87*, 1377.
- (7) Hayakawa, K.; Kwak, J. C. T. In *Cationic Surfactants*; Surfactant Science Series; Rubingh, D. N., Holland, P., Eds.; Marcel Dekker: New York, 1991; Vol. 37, Chapter 5, p 189.
- (8) Anthony, O.; Zana, R. *Langmuir* **1994**, *10*, 4048.
- (9) Saito, S.; Kitamura, K. *Tenside Deterg.* **1981**, *18*, 117.
- (10) Fundin, J.; Brown, W. *Macromolecules* **1994**, *27*, 5024.
- (11) Feitosa, E.; Brown, W.; Hansson, P. *Macromolecules*, **1996**, *29*, 2169.
- (12) Schillén, K.; Brown, W.; Johnsen, R. M. *Macromolecules* **1994**, *27*, 4825.
- (13) Provencier, S. W. *Makromol. Chem.* **1979**, *180*, 201.
- (14) Jakes, J. *Czech. J. Phys.* **1988**, *B38*, 1305.
- (15) Johnsen, R. M.; Brown, W. In *Laser Light Scattering in Biochemistry*; Harding, S. E., Sattelle, D. B., Bloomfield, V. A., Eds.; Royal Society of Chemistry: London, 1992; p 77.
- (16) Almgren, M.; Alsins, J.; van Stam, J.; Mukhtar, E. *Prog. Colloid Sci.* **1988**, *76*, 68.
- (17) Almgren, M.; Löfroth, J.; van Stam, J. *J. Phys. Chem.* **1986**, *90*, 4431.
- (18) Almgren, M.; Hansson, P.; Mukhtar, E.; van Stam, J. *Langmuir* **1992**, *8*, 2405.
- (19) Almgren, M. In *Kinetics and Catalysis in Microheterogeneous Systems*; Gratzel, M., Kalyanasundaram, K., Eds.; Marcel Dekker: New York, 1991; p 63.
- (20) Almgren, M. *Adv. Colloid Interface Sci.* **1992**, *41*, 9.
- (21) Zana, R. In *Surfactants in Solution. New Methods of Investigation*; Surfactant Science Series; Vol. 22, Marcel Dekker: New York, 1987; Vol. 22, p 241.
- (22) Infelta, P. P.; Grätzel, M.; Thomas, J. K. *J. Phys. Chem.* **1974**, *78*, 190.
- (23) Almgren, M.; Alsins, J. *Prog. Colloid Polym. Sci.* **1987**, *74*, 55.
- (24) Nilsson, P. G.; Wennerström, H.; Lindman, B. *J. Phys. Chem.* **1983**, *87*, 1377.
- (25) Kato, T.; Anzai, S.; Seimiya, T. *J. Phys. Chem.* **1987**, *91*, 4655.
- (26) Karlström, G. *J. Phys. Chem.* **1985**, *89*, 4962.
- (27) Thalberg, K.; van Stam, J.; Lindblad, C.; Almgren, M.; Lindman, B. *J. Phys. Chem.* **1991**, *95*, 8975.
- (28) van Stam, J.; Brown, W.; Fundin, J.; Almgren, M.; Lindblad, C. In *Colloid–Polymer Interactions. Particulate, Amphiphilic and Biological Surfaces*; Dubin, P., Tong, P., Eds.; American Chemical Society: Washington, DC, 1993; p 195.
- (29) van Stam, J.; Almgren, M.; Lindblad, C. *Prog. Colloid Polym. Sci.* **1991**, *84*, 13.
- (30) Winnik, F. M. *Langmuir* **1990**, *6*, 522.
- (31) Fundin, J.; Hansson, P.; Brown, W.; Idegran, I. *Macromolecules*, submitted.